ISME2013-715

On the Development of a Numerical Model for Liquid Sloshing in Containers

Alireza Javanshir[1], Rasoul Elahi[2] and Mohammad Passandideh-Fard[3]

[1] Graduate Student, Ferdowsi University of Mashhad; ajavanshir19@yahoo.com
[2] Graduate Student, Ferdowsi University of Mashhad;r.elahi.msc@gmail.com
[3] Associate Professor, Ferdowsi University of Mashhad; mpfard@um.ac.ir

Abstract
In this paper, a two-dimensional numerical model is developed to study liquid sloshing in containers in presence of liquid free surface deformation, liquid viscosity and surface tension. The model is validated by a comparison between the computational and theoretical/experimental results for time-dependent linear/angular acceleration sloshing scenarios. The governing equations for the 2D incompressible fluid flow are continuity and Navier-Stokes equations along with an equation for the free surface advection. The deformation of the liquid-gas interface is modeled using the Volume-of-Fluid (VOF) method. The fluid flow equations describing the fluid sloshing in the container and the dynamic equation which describes the movement of the container are solved separately in two coupled programs. In each time step of computations, the outputs of the fluid program (forces and torque) are obtained and used as inputs for the dynamic program. The forces and torque are applied to the body of the container resulting in translational and rotational accelerations which are then used as inputs to the fluid program. The model is also used to simulate the movement of the liquid container in a general case where a complete interaction between liquid and solid body of the container exits and the container has both linear and rotational accelerations.

Keywords: liquid sloshing-numerical simulation-Volume of Fluid

Introduction

The sloshing phenomenon occurs in many applications, such as, propellant tank in aerospace devices and LNG (liquid natural gas) cargos in the ship industry. When an external transient or steady force acts on a fluid, the liquid is driven from equilibrium state. In this condition, the free surface of the liquid moves and the liquid splash on the container walls. In many cases, these forces affect the maneuver of the vehicle. The influence of sloshing liquid may hamper critical maneuvers in space, such as the docking of liquid-cargo vehicles or the pointing of observational satellites. Several serious problems with sloshing liquid in a spacecraft have been reported over the years. For example, during the last seconds of the first lunar landing [1], or another example is the NEAR (Near Earth Asteroid Rendezvous) mission to the asteroid Eros in 1998 [2]. During an orbital correction, the spacecraft experienced an unexpected motion; fuel slosh was identified as the probable cause [2].

The Marker-and-Cell (MAC) method is the 'father' of all free-surface flow methods [3]; it makes the use of mass-less particles to keep track of the liquid region. Accuracy requires a considerable number of particles per grid cell, making the method computationally expensive, especially in 3D. A cheaper way is to apply only surface markers [4], but now splitting and merging of the surface are difficult to handle. The MAC follow-up is the volume-of-fluid (VOF) method introduced by Hirt and Nichols [5]. Here a discrete indicator (or color) function is used that corresponds to the cell volume occupied by fluid. This method was improved considerably by Young [6] who modeled the free surface by Piecewise Linear Interface construction (PLIC) Algorithms.

Sloshing phenomenon in a rectangular tank has been intensively studied in the last few decades. Many researchers have devoted their efforts to study sloshing analytically based on potential flow theory. For example, Faltinsen [7] derived a linear analytical solution for liquid sloshing in a horizontally excited 2D rectangular tan; this solution has been widely used in the validation of numerical models. Recently, Faltinsen et al. [8] and Faltinsen and Timokha [9] developed a multimodal approach to describe the non-linear sloshing in a rectangular tank with a finite water depth. Later, Hill [10] analyzed the transient behavior of the resonated waves by relaxing many of the assumptions adopted in the previous studies. However, these theoretical analyses are not valid for viscous and turbulent flows, therefore, the overturning and breaking waves during violent liquid sloshing cannot be described. On the other hand, laboratory measurements of wave height and hydrodynamic pressure have been reported by Verhagen and Wijingaarden [11], Okamoto and Kawahara [12, 13], and Akyildiz and U¨nal [14]. These measurements are very useful for validating theoretical solution and numerical results.

The numerical modeling is one of the viable methods in studying nonlinear free-surface wave and estimating the magnitude and location of the impulsive pressure acting on the tank walls. Nowadays, it is not extraordinary to use numerical methods for simulation of the nonlinear waves interacting with the structure like Mo and Liu [15] and Seung-Hee Lee et al. [16]. Shao et al. [17] used the SPH (Smoothed particle hydrodynamics) method for simulating the liquid sloshing. Accordingly, numerical methods can be

employed in sloshing analyses to reduce the number of required experiments.

The above-mentioned studies considered a one-way interaction between liquid and solid body; i.e., the solid-body movement was enforced in the simulations. Veldman [6] was the first who considered a two-way liquid/solid interaction model to study the sloshing phenomenon. In his model, however, the gas phase was not considered in the solution.

In the previous studies some assumptions such as two-phase flow and violent sloshing moving and liquid effect on solid body weren't considered. In this paper, a two-dimensional numerical model is developed to study liquid sloshing in containers in presence of liquid free surface deformation, liquid viscosity and surface tension and those assumptions are considered. The model is validated by a comparison between the computational and theoretical/experimental results for time-dependent linear/angular acceleration sloshing scenarios. The deformation of the liquid-gas interface is modeled using the Volume-of-Fluid (VOF) method. The model is also used to simulate the movement of the liquid container in a general case where a complete interaction between liquid and solid body of the container exits and the container has both linear and rotational accelerations.

Mathematical Model

Fluid dynamics

The governing equations are the unsteady, incompressible, continuity and Navier–Stokes equations. The fluid motion is described by means of the conservation of mass [6]:

$$\nabla \cdot \vec{V} = 0 \tag{1}$$

and conservation of momentum:

$$\frac{\partial \vec{V}}{\partial t} + \left(\vec{V} \cdot \nabla\right)\vec{V} = -\frac{1}{\rho}(\nabla p - \mu\left(\nabla \cdot \nabla\right)\vec{V} + \vec{F_B} + \vec{F_v} \tag{2}$$

where $\vec{V}$ denotes the velocity of the fluid relative to the tank, p the pressure, ρ and μ the fluid density and viscosity, respectively. The vectors $\vec{F_B}$ and $\vec{F_v}$ represent the external body force and a virtual body force induced by the motion of the tank. In the Volume of Fluid (VOF) method, the free surface deformation is characterized by means of a scalar function, *f*, whose value is set based on the volume fraction of a cell occupied by liquid. The equation governing *f* is:

$$\frac{Df}{Dt} = \frac{\partial f}{\partial t} + \vec{V} \cdot \vec{\nabla} f = 0 \tag{3}$$

This equation along with the Young PLIC algorithm [6] is used to track the location of the interface. For boundary conditions, the usual no-slip condition for viscous flow is applied at the tank wall. More details of the model are given elsewhere [18].

Solid-body dynamics

The model for solid-body motion consists of an equation for linear momentum [17].

$$m_s \vec{\dot{q}} + \vec{\dot{\omega}} \times m_s \vec{r}_s + \vec{\omega} \times \left(\vec{\omega} \times m_s \vec{r}_s\right) = \vec{R} + m_s \vec{F_B} \tag{4}$$

and an equation for angular momentum

$$m_s \vec{r}_s \times \vec{\dot{q}} + I_s \vec{\dot{\omega}} + \vec{\omega} \times \left(I_s \vec{\omega}\right) = \vec{T} + m_s \vec{r}_s \times \vec{F_B} \tag{5}$$

In these equations, $\vec{\dot{q}}$ (linear acceleration) and $\vec{\dot{\omega}}$ (angular acceleration) are unknown variables. The mass of the solid body is denoted by m_s; further, I_s is the moment of inertia tensor and $\vec{r}$ is the center of mass of the solid. The last terms in Equations 4 and 5 represent the force and torque due to an external body force such as gravity. Finally, $\vec{R}$ and $\vec{T}$ are, respectively, the force and torque that the fluid, via pressure and viscous effects, exerts on the boundaries of the solid body. $\vec{R}$ and $\vec{T}$ are defined as:

$$\vec{R} = \oint_{\partial V} (pI_3 - \mu \nabla \vec{V}).nds \tag{6}$$

$$\vec{T} = \oint_{\partial V} (r \times (pI_3 - \mu \nabla \vec{V})).nds \tag{7}$$

Here, I_3 is the 3×3 identity matrix and n the outward pointing normal to the boundary of volume ∂V of the solid body.

Virtual body force method

In order to couple the fluid dynamics and solid-body dynamics, the motion of the fluid in presence of the solid body movement has to be modeled. Here, the fluid velocity is considered in two reference frames: the velocity $\vec{V^*}$ of a fluid particle with respect to an inertial reference frame and the velocity $\vec{V}$ of the same liquid particle with respect to a moving reference frame. The relation between $\vec{V^*}$ and $\vec{V}$ is given by

$$\frac{D\vec{V^*}}{Dt} = \vec{\dot{q}} + \vec{\dot{\omega}} \times \vec{r} + \vec{\omega} \times \left(\vec{\omega} \times \vec{r}\right) + \frac{D\vec{V}}{Dt} + 2\vec{\omega} \times \vec{V} \tag{8}$$

where $\vec{\dot{q}} = \frac{d\vec{q}}{dt} + \vec{\omega} \times \vec{q}$ is the acceleration of the moving origin with respect to the origin of the inertial reference frame; $\vec{\dot{\omega}}$, $\vec{\omega}$ and $\vec{r}$ are the angular acceleration ,angular velocity and the position vector of the liquid particle respectively and they are in the moving reference frame. The third and fifth terms in the right-hand side of Equation 8 represent the centrifugal and Coriolis accelerations respectively. Now, the Navier-stokes equations become:

$$\frac{D\vec{V^*}}{Dt} = -\frac{1}{\rho}\left(\nabla p - \mu\left(\nabla \cdot \nabla\right)\vec{V}\right) + \vec{F_B} \tag{9}$$

Alternatively, using Equation 9:

$$\frac{D\vec{V}}{Dt} = -\frac{1}{\rho}\left(\nabla p - \mu\left(\nabla \cdot \nabla\right)\vec{V}\right) + \vec{F_B} + \vec{F_v} \tag{10}$$

where

$$\vec{F_V} = -\vec{\dot{q}} - \vec{\dot{\omega}} \times \vec{r} - \vec{\omega} \times \left(\vec{\omega} \times \vec{r}\right) - 2\vec{\omega} \times \vec{V} \tag{11}$$

Equation 10 has a form similar to Equation 2 (meaning that in the numerical model for the liquid dynamics only small changes are required). Using Newton's third law, the extra term $\vec{F_v}$ in Equation 10 can be seen as acceleration due to a virtual body force. Instead of actually moving the solid body in the numerical model, the fluid is subjected to an acceleration (equal in magnitude and opposite in sign) to account for the solid-body motion. Considering

Equations 10 and divergence theorem, Equations 6 and 7 will transform into:

$$\vec{R} = \oiint_V \left(\nabla p - \mu\left(\nabla\cdot\nabla\right)\vec{V}\right)dV = -\oiint_V \rho\left(\frac{D\vec{V}}{Dt} - \overrightarrow{F_B} - \overrightarrow{F_v}\right)dV \quad (12)$$

$$\vec{T} = \oiint_V \vec{r}\times\left(\nabla p - \mu\left(\nabla\cdot\nabla\right)\vec{V}\right)dV = -\oiint_V \rho r\times\left(\frac{D\vec{V}}{Dt} - \overrightarrow{F_B} - \overrightarrow{F_v}\right)dV \quad (13)$$

Direct time integration of Equations 4 and 5 would result in a method that is not stable for arbitrary liquid/solid mass ratios. Thus, the system for the solid-body dynamics is rewritten first. Veldman [17] introduced a new coupling method that is computationally stable. In his model, Equations 4 and 5 are rewritten as:

$$m\dot{\vec{q}} + \dot{\vec{\omega}}\times m\bar{r} + \vec{\omega}\times\left(\vec{\omega}\times m\bar{r}\right) = \oiint_V \rho\left(\frac{D\vec{V}}{Dt} + 2\vec{\omega}\times\vec{u} - \overrightarrow{F_B}\right)dV + m_s\overrightarrow{F_B} \quad (14)$$

$$m\bar{r}\times\dot{\vec{q}} + I\dot{\vec{\omega}} + \vec{\omega}\times\left(I\vec{\omega}\right) = \oiint_V \rho r\times\left(\frac{D\vec{V}}{Dt} + 2\vec{\omega}\times\vec{u} - \overrightarrow{F_B}\right)dV + m_s\bar{r}\times\overrightarrow{F_B} \quad (15)$$

In these equations $m = m_S + m_L$ is the total mass and $I = I_S + I_L$ the moment-of-inertia tensor of the coupled system. The centre of mass of the coupled system is denoted by

$$r = \frac{m_S\bar{r}_s + m_l\bar{r}_l}{m} \quad (16)$$

An important difference between the left hand sides of Eqs. 4 and 14 (and similarly between Eqs. 5 and 15) is the distribution of the solid-body mass and the liquid mass over the left-hand side and right-hand side of the equations.

Numerical Method

VOF algorithm

The finite difference discretisation of the governing equation follows the Euler forward scheme in a staggered grid [19].

$$\frac{\vec{V}^{n+1} - \vec{V}^{n}}{\delta t} = -(\vec{V}\cdot\vec{\nabla}\vec{V})^n - \frac{1}{\rho^n}\vec{\nabla}p^{n+1} - \frac{1}{\rho^n}\vec{\nabla}\cdot\vec{\tau}^n + \frac{1}{\rho^n}\overrightarrow{F_B}^n \quad (17)$$

In the above equation, all terms except for pressure are computed explicitly. The velocity field is calculated according to a two-step projection method as follows. First, an intermediate velocity $\vec{\vec{V}}$ is obtained,

$$\frac{\vec{\vec{V}}^{n} - \vec{V}^{n}}{\delta t} = -(\vec{V}\cdot\vec{\nabla}\vec{V})^n - \frac{1}{\rho^n}\vec{\nabla}\cdot\vec{\tau}^n + \frac{1}{\rho^n}\overrightarrow{F_B}^n \quad (18)$$

The CSF method is used to model surface tension as a body force $\overrightarrow{F_B}$ that acts only on interfacial cells. In the second step, the intermediate velocity is projected to a divergence free velocity field:

$$\frac{\vec{V}^{n+1} - \vec{\vec{V}}^{n}}{\delta t} = -\frac{1}{\rho^n}\vec{\nabla}p^{n+1} \quad (19)$$

The continuity equation is also satisfied for the velocity field at the new time step:

$$\vec{\nabla}\cdot\vec{V}^{n+1} = 0 \quad (20)$$

Solid dynamic system

In this section, the discretization of Equations 14 and 15 is discussed in more detail. The temporal discretization of the equations for linear momentum (Equation 14) and angular momentum (Equation 15) is straight forward. Both $\frac{d\vec{q}}{dt}$ and $\frac{d\vec{\omega}}{dt}$ are discretized at the new time level (indicated by superscript $n+1$). The linear and angular velocities are discretized at the old time level (indicated by a superscript *n*). Since the model for the solid-body dynamics is applied after the model for the liquid dynamics has been completed (in the same time step), all the quantities from the liquid model carry a superscript $n+1$.

$$m\frac{d\vec{q}^{n+1}}{dt} + \frac{d\vec{\omega}^{n+1}}{dt}\times m\bar{r}^{n+1} = \overrightarrow{\Phi^n} \quad (21.a)$$

$$m\bar{r}^{n+1}\times\frac{d\vec{q}^{n+1}}{dt} + I^{n+1}\frac{d\vec{\omega}^{n+1}}{dt} = \overrightarrow{\xi^n} \quad (21.b)$$

where

$$\overrightarrow{\Phi^n} = -m\overrightarrow{\omega^n}\times\overrightarrow{q^n} - \overrightarrow{\omega^n}\times\left(\overrightarrow{\omega^n}\times m\bar{r}^{n+1}\right) - \oiint_V \rho\vec{\Psi}^{n+1}dV + m_s\overrightarrow{F_B}^{n+1} \quad (22)$$

$$\overrightarrow{\xi^n} = -m\vec{r}^{n+1}\times(\overrightarrow{\omega^n}\times\overrightarrow{q^n}) - \overrightarrow{\omega^n}\times I^{n+1}\overrightarrow{\omega^n} - \oiint_V \rho\vec{\Psi}^{n+1}dV + m_s\overrightarrow{F_B}^{n+1} \quad (23)$$

In these equations

$$\vec{\Psi}^{n+1} = \frac{D\vec{V}^{n+1}}{Dt} + 2\vec{\omega}^n\times\vec{V}^{n+1} - \overrightarrow{F_B}^{n+1} \quad (24)$$

In order to solve the system of Equations 21, in matrix form the 3×3 linear system (21) for the unknown vectors $\left(\frac{dq}{dt}\right)^{n+1}$ and $\left(\frac{d\omega}{dt}\right)^{n+1}$ reads

$$\begin{pmatrix} m & 0 & -m\bar{r}_y \\ 0 & m & m\bar{r}_x \\ -m\bar{r}_y & m\bar{r}_x & I_{zz} \end{pmatrix}\begin{pmatrix} dq_x/dt \\ dq_y/dt \\ d\omega_z/dt \end{pmatrix} = \begin{pmatrix} \Phi_x \\ \Phi_y \\ \xi_z \end{pmatrix} \quad (25)$$

In this equation, the superscripts have been dropped (it is clear that the matrix and the right-hand side vector are evaluated at time level *n*, while the unknown vector contains quantities at time level $n+1$). By solving the system of Equations 25, the accelerations $\left(\frac{dq_x}{dt}, \frac{dq_y}{dt}, \frac{d\omega}{dt}\right)$ are obtained at the new time level. After calculating accelerations, the velocities and container displacement are obtained.

Results and Discussion

Model Validation

In order to validate the model in simulating liquid sloshing, first, a few test cases are considered for which analytical or experimental results are available. These cases include: oscillating tank ,container under linear acceleration and rotating tank.

As a first test case In order to evaluate the performance of the model in simulating free surface flows under time dependant acceleration , a test case was considered and the results were compared with available experimental data. A rectangular tank of 0.4 m wide and 0.2 m high, filled with 60 percent of water (0.12 m high) , was forced to oscillate from left to right. The water began to move in an oscillatory manner before impacting the top wall. Experimental free surface shapes [20] are available prior to the first impact on the top wall (Figure 1). The tank was moved in a horizontal plane as follows:

$$x(t) = A_0 \left\lfloor sin(2\pi f_1 t) - sin(2\pi f_2 t) \right\rfloor \quad (26)$$

$$A_0 = 0.0075m, f_1 = 1.598Hz, f_2 = 1.307Hz$$

As can be seen in Figure 1 computed free surface shapes are in good agreement with those obtained from experiments (black dots) [20]. However, at t=1.23s it can be seen small differences between numerical results and experimental data for the free surface shape. This difference can be attributed to the 2D modeling instead of the real 3D nature of sloshing phenomenon. Furthermore, for this simulation it was considered an equilibrium contact angle on the container walls whereas in reality the contact angle must be dynamic.

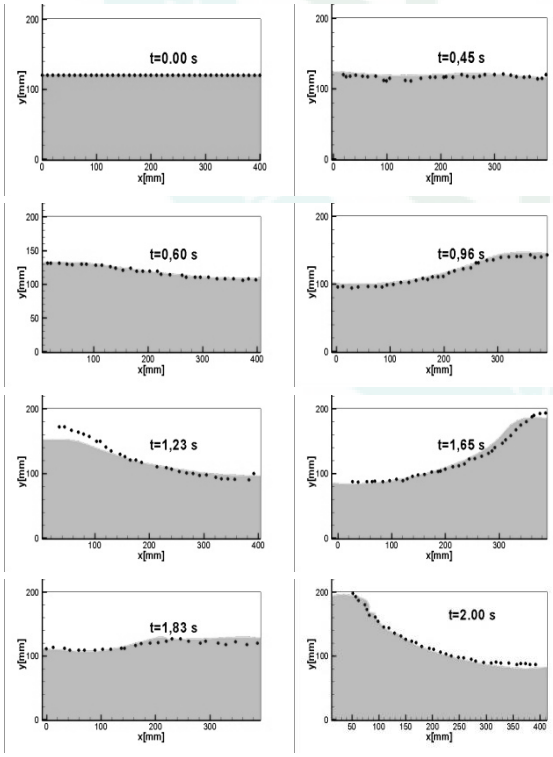

Fig. 1: A comparison between numerical (grey area) and experimental (black dots) free surface shape [20].

As a second test case, a container under linear acceleration considered and the results were compared with available theoretical data. A 25×25 centimeters rectangular container was considered and this allows for approximately 62.5 liters fuel. The container was almost 25% (15.6 liters) filled with fuel and It was assumed that the vehicle was at rest at time equal zero then it started to move along the x-direction with a constant acceleration equal to $4.5 m/s^2$. The fuel inside the container was assumed to have the property of water. The liquid was deviated from equilibrium state and moved and clashed with the wall of the container. After a while, the liquid neared a stable condition at a certain angel. In this study, we compare the results of this simulation with the available theoretical data. Based on the theory, the free surface of liquid must be perpendicular to the pressure gradient and is thus tilted at a downward angle θ such that:

$$\theta = \arctan\left(\frac{a_x}{a_y + g}\right) \quad (27)$$

Where a_x, a_y and g are uniform acceleration in x and y-direction and gravity acceleration respectively. In this study the free surface tilts at an angle of 24.64 deg, regardless of the shape of the container. In Figure 2, the free surface deformation is shown at different times. In this figure, the theoretical tilt angle is represented with a dash line. As can be seen, computed free surface shapes at the steady state condition (t=10s) are in good agreement with those obtained from Equation 27 (dash line).

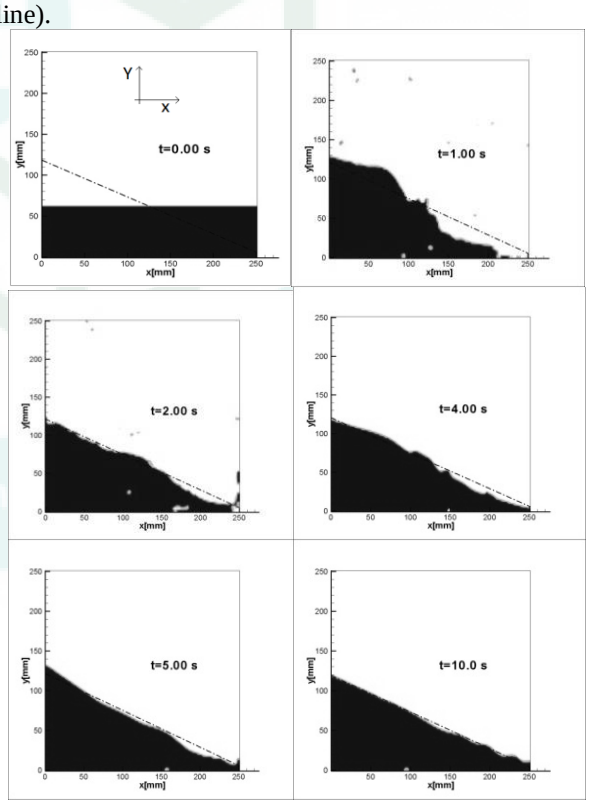

Figure 2: Liquid sloshing in a container that undergoes a linear acceleration equal to 4.5m/s^2 in the x direction.

As third test case in order to validate the numerical model for rotational motion and the effects of centrifugal force, a square container with 100mm side

was considered. The container was filled up to 15mm of water. It was assumed that the container was at rest at equal zero and after a very short time it starts to rotate around left bottom corner (Figure 3) with a constant angular velocity equal to $2\pi\ rad/s$. In this case the gravity force was not considered, thus there was not any linear acceleration. Because of the centrifugal force reaction, the fluid particles moved to furthest location from the rotating origin with acceleration equal to $r\omega^2$. The steady shape of liquid is the arc of the circle such that the radius of the circle can be obtained theoretically. Figure 3 show the result of this investigation. In this Figure the dash circle line indicates the theoretical free surface. As can be seen the steady shape of liquid free surface has good agreement with theoretical circle line.

As seen in these three cases, the results show that this method has a rational validation with theoretical/experimental results, thus it can be used for more complex cases such as rolling tank and ferris wheel motion.

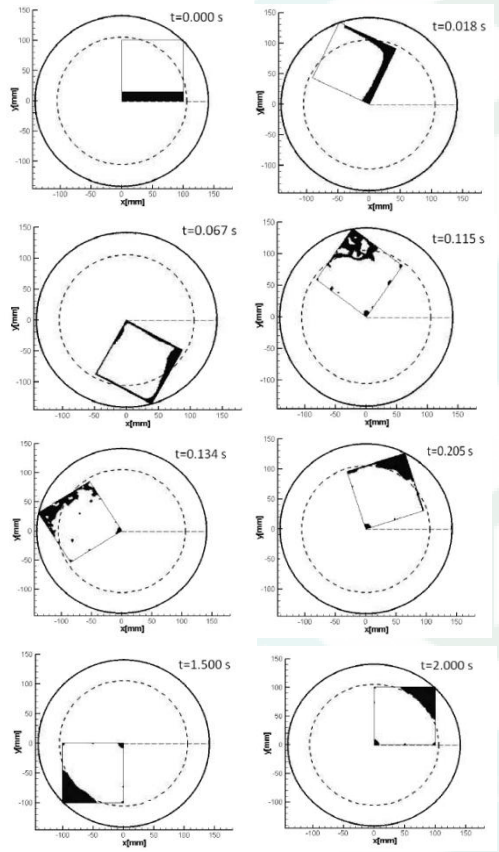

Figure 3: Liquid sloshing in the container under the centrifugal force reaction.

Rolling tank

Having validated the model for linear and angular motions separately, a test case is considered for which the combination of both motions exists. In this simulation, a square container 100mm in side is filled partially with water up to 15 mm from the bottom as seen in Figure 4. The container is then forced to roll clockwise on its sides (see Figure 4) such that the center of the container has a π rad/s uniform angular velocity. The free surface deformation in this complex motion is illustrated at Figure 4.

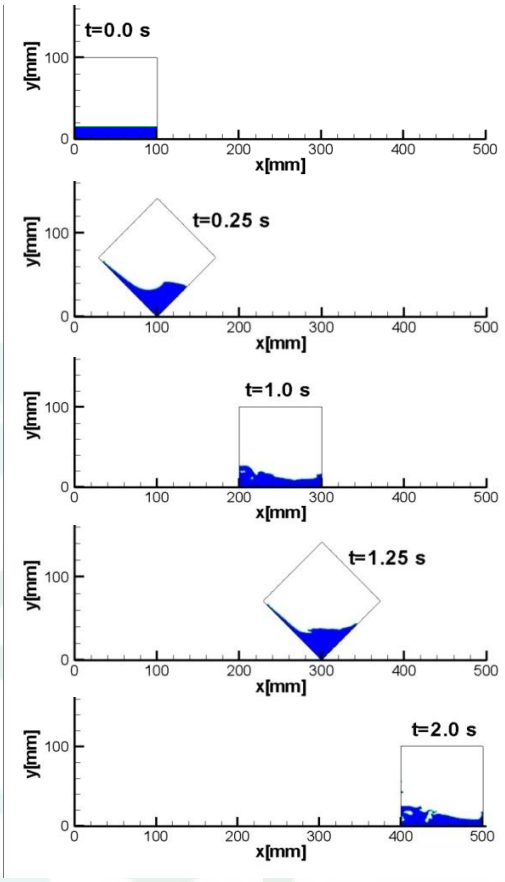

Figure 4: Liquid sloshing in the rolling container

As can be seen the gravity force act as a damping force in sloshing phenomena that caused the bulk of the fluid always be at the bottom of the container.

Ferris wheel motion

The final case considered in this paper is that of a ferris wheel motion where a complete fluid/solid interaction exists. This case includes the time dependent linear acceleration in both *x* and *y* directions. Because of the solid-liquid interaction, the container is allowed to rotate freely. A square container, 100mm in side and filled 25% with a square shape water portion, is hanged from the top corner at time t=0 as shown in Figure 5. This corner is pined to the circumference of a wheel with 200mm in radius. At t=0, the pin point start to rotate around the center of the circle with a constant angular velocity (π rad/s). The bulk of the liquid clashes with the container walls where it exchanges forces with the solid container. As a result the container rotates around the pin point freely. Also in order to show the solid-liquid interaction, the low weight container was selected (0.004kg).

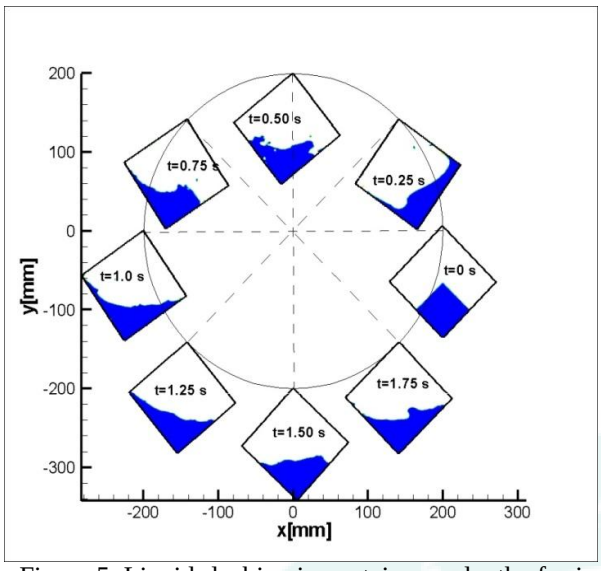

Figure 5: Liquid sloshing in container under the ferris wheel motion

As can be seen in Figure 5 the container experienced the rotating movement.

Conclusions

In this study, we have developed a computational model that can simulate liquid sloshing in 2D containers and fuel tanks with angular and translational movement including linear/angular acceleration. The code can be used for determining the forces and torques that are exerted to the structure of the vessels or the containers due to the sloshing waves. The model was validated by a comparison between the computational and theoritical results and timed dependent acceleration. The deformation of the liquid-gas interface is modeled using the Volume-of-Fluid (VOF) method. Finally,the liquid intercation on sloid body was investigated and thus this code was developed and used for any movement.

References

[1] Apollo 11 Lunar Surface Journal, "The first lunar landing mission time". On the WWW,at http://www.hq.nasa.gov/office/pao/History/alsj/a11/a11.landing.html.

[2] NEAR Anomaly Review Board, 1999. "The NEAR Rendezvous Burn Anomaly of December 1998", Johns Hopkins University, Applied Physics Laboratory.

[3] Harlow, F.H., Welch, J.E.,1967 . "Numerical calculation of time-dependent viscous incompressible flow of fluid with free surface". Phys. Fluids, 2182–2189.

[4] Juric, D., Tryggvason, G., 1996. "A front tracking method for dendritic solidification". J. Comput. Phys, 127–148.

[5] Hirt, C.W., Nichols, B.D., 1981. "Volume of fluid (VOF) method for the dynamics of free boundaries". J. Comput. Phys. 201–225.

[6] Veldman, A.E.P., Gerrits, J., Luppes, R., Helder, J.A., Vreeburg, J.P.B., 2007. "The numerical simulation of liquid sloshing on board spacecraft". J. Comput. Phys., Vol. 224, 82-99.

[7] Faltinsen, O.M., 1978. "A numerical nonlinear method of sloshing in tanks with two-dimensional flow". J. Ship Res. 22 (8) 193–202.

[8] Faltinsen, O.M., Rognebakke, O.F., Lukovsky, I.A., Timokha, A.N., 2000. "Multidimensional modal analysis of nonlinear sloshing in a rectangular tank with finite water depth". J. Fluid Mech. 407 (2000) 201–234.

[9] Faltinsen, O.M., Timokha, A.N., 2001."Adaptive multimodal approach to nonlinear sloshing in a rectangular tank". J. Fluid Mech. 432 (2)167–200.

[10] Hill, D.F., 2003. "Transient and steady-stateamplitudes of forced waves in rectangular basins". Phys.Fluid15-1576–1587.

[11] Verhagen, H.G., Wijingaarden, L., 1965. "Non-linear oscillation of fluid in a container".J. Fluid Mech. 22 - 737–751.

[12] Okamoto, T., Kawahara, M., 1990. "Two-dimensional sloshing analysis by Lagrangian finite element method", Int. J. Numer. Method Fluid11 - 453–477.

[13] Okamoto, T., Kawahara, M., 1197. "3-D sloshing analysis by an arbitrary Lagrangian–Eulerian finite element method", Int. J. Comput. FluidDyn. 8 - 129–146.

[14] Akyildiz, H. Unal, E., 2005."Experimental investigation of pressure distribution on a rectangular tank due to the liquid sloshing". Ocean Eng.1503–1516.

[15] Mo, W., Liu, P.L., 2009. "Three dimensional numerical simulations for non-breaking solitary wave interaction with a group of slender vertical cylinders". International Journal of Naval Architecture and Ocean Engineering 1 (1), 20–28.

[16] Hee Lee, Seung-, GillLee, Young- , Kwang-LeolJeong, 2011. "Numerical simulation of three-dimensional sloshing phenomena using a finite difference method with marker-density scheme". Ocean Engineering 38 - 206–225.

[17] Shao, J.R., Li, H.Q., Liu, G.R., 2012. "An improved SPH method for modeling liquid sloshing dynamics". J. Computers and Structures, 100-101–26.

[18] Mirzaii, I., Passandideh-Fard, M., 2012. " Modeling free surface flows in presence of an arbitrary moving object". International Journal of Multiphase Flow 39 - 216–226.

[19] Passandideh-Fard, M., Roohi, E., "Transient simulations of cavitating flows using amodified volume-of-fluid (VOF) technique". J. Computational Fluid Dynamics vol22:1, 97 – 114.

[20] Corrignan, P., 1994. " Analyse Physique des Phénoménes Associés au Ballotement de Liquide dans des Réservoirs (Sloshing)", Ph.D. thesis, Ecole Centrale de Nantes.